Deep Mining 2024 – P Andrieux & D Cumming-Potvin (eds)

doi:10.36487/ACG_repo/2465_38

Ground support condition monitoring through point cloud analytics

Amit Patwardhan [a,*], Ramin Karim [a]

[a] *Division of Operation, Maintenance and Acoustics, Luleå University of Technology, Sweden*

Abstract

This paper presents a methodology and the results of workflow developed to process point cloud data from underground drifts for condition monitoring of ground support. The workflow focuses on extraction and comparison of information of individual rockbolts and rockbolt neighbourhood prior to, and following, recorded seismic events. Data sources used in this methodology are point cloud data resulting from mobile LiDAR scanning and event data of blasting and microseismic events. In the first step of the workflow, locations in the drift with recorded microseismic events in the vicinity are selected. In the second step, LiDAR scans performed before and after the occurrence of one or more natural or man-made events are used to extract point cloud data within a region close to the recorded events. The extracted point cloud data is processed to compute information about the rockbolts. For each detected rockbolt, the following information is extracted: position on drift surface, tip position, angle to drift surface, length, neighbouring rockbolts, and rockbolt to neighbour's distances. In the next phase, the rockbolt information extracted from two or more scans over the period encompassing the event are analysed. Corresponding rockbolt information from pre-event and post-event point cloud data are used to compute variation in rockbolt features. The computed variations are examined statistically and used to create a visualisation for decision support to be used by rock mechanics engineers and surveyors.

Keywords: *ground support, condition monitoring, point cloud*

1 Introduction

Deep mining is a key enabler for long-term growth. The process of deep mining depends on creation of drifts through the process of drilling, blasting, loading, hauling, scaling, etc. allowing access to the orebody. The process of excavation rearranges the stresses near the void, which may lead to deformation. The convergence is generally less than the critical threshold of ~1% (10 cm in 10 m diameter) (Sakurai 1984). To retain the convergence within critical limits, the rock mass is reinforced to conserve the inherent strength and make the excavation self-supporting (Li 2017). Reinforcement is provided through ground support, with the aim of stabilising the rock masses. Rockbolts are a widely used support element in underground mines and civil tunnels (Li 2017). Deformation may tear the plate while the rockbolt remains intact or the bolt may lose its capacity and may move under gravity (Simser 2007). Continual evaluation of deformation is critical for maintaining safety.

Conventional instruments for geomechanics monitoring work on a point-to-point basis, hence spatially continuous displacement data acquisition and monitoring is challenging (Jones 2020). LiDAR mapping technology developed through laser scanning has improved over the years in terms of scan resolution and accuracy. Today, LiDAR is being used in varied fields like detection of forest cover, mapping of archaeological sites, urban planning, study of geomechanics and, more recently, self-driving cars (Fernandes et al. 2021; Poux et al. 2017; Romero-Jarén & Arranz 2021; Xue et al. 2020). LiDAR provides a fast and efficient method

* Corresponding author. Email address: amit.patwardhan@ltu.se

of 3D spatial data collection over a large area through static or mobile scanning. Mobile scanning can be performed by carrying the device by hand or mounting it on a vehicle, drone, or robot.

LiDAR has been in use for terrestrial monitoring in the geographical information systems, it was extended to mining, and has been used for accurate surveying, volume and mass calculation, true-to-scale map generation, and asset inventory generation, providing data economically in terms of time and manpower. Data collection and processing has improved rock face monitoring, slope stability monitoring, deformation, and to understand long-term trends in rock behaviour (Gigli & Casagli 2011; Leottau et al. 2020; Walton et al. 2018; Yu et al. 2011, 2010).

As one of the applications of extraction of information from underground tunnel point cloud data, researchers have targeted the problem of extraction of rockbolt information (Gallwey et al. 2020; Li et al. 2022; Martínez-Sánchez et al. 2016; Saydam et al. 2021; Singh et al. 2021a, 2021b). The modality followed in most of the techniques developed by researchers follows the path of noise filtering, uniform down sampling, extracting point-based features based on eigenvalues (Weinmann et al. 2017) and fast point feature histograms (Rusu et al. 2009) and training neural network or random forest classifiers, clustering and finally applying a cluster evaluator to extract rockbolt point cloud data. Use of extracted rockbolt information has seen limited application and has been used only for registration of two or more scans for comparison of the surface shotcrete coating (Martínez-Sánchez et al. 2016).

To quantify the change in surface over a period, comparative measurement of surfaces between two point cloud data sets is required. This problem has been addressed for comparison of terrestrial surfaces through Multiscale Model to Model Cloud Comparison (M3C2) (Lague et al. 2013). To quantify the effect of tunnel deformation, the algorithm must be adapted to the tunnel design.

Data processing software should have the functionality to understand the specific requirements (3D spatial data) to process and extract information useful to the domain experts. Hence, effort towards development of algorithms and software for processing of point cloud data for analysis and automation can facilitate making more informed decisions. Further, point cloud data analysis requires that the alignment between the primary and secondary scans are sufficiently accurate and the analysis should show the magnitude of movement and distinguish between convergence and divergence (Jones & Beck 2018).

In this paper we address condition monitoring of rockbolts using point cloud data by addressing the following gaps:

1. Extraction of rockbolt information in regions with high density non-rockbolt items including meshes and steel ribs.
2. Quantification of deformation and error correction based on local registration error between the compared scans.
3. Visualisation of magnitude of movement between the compared scans and indicators for convergence and divergence.

2 Method

This section describes the steps carried out for extraction, processing and visualisation of rockbolts for performing condition monitoring. LiDAR scanning and surveying is carried out at regular intervals resulting in data used for processing. The complete processing pipeline is developed in Python programming language using open-source tools and libraries such as Open3D (Harris et al. 2020; Van Rossum 1995; Zhou et al. 2018). In the first stage, processing of the point cloud extracts the information about the rockbolts. In the second stage, the extracted rockbolt information from two consecutive point clouds is analysed to compare the rockbolts information. Finally, in the third stage, visualisations to represent the computed results are generated for decision support.

2.1 Region of interest selection

The entire region of underground tunnels may not be of interest for continual inspections. Such inspection will affect the production process due to survey requirements and will require a high amount of both computation and data management. A region of interest can be selected based on mine engineer's experience and observations. In addition and in this paper, available data sources such as blasting times and microseismic events have been used to locate the region of interest.

In this paper, the region of interest is an intersection point of three tunnels. This region has been selected due to the recorded microseismic activity under the tunnel, four hours after the blasting was carried out in one of the connected tunnels. The selected region is approximately 6 × 6 × 6 m in dimensions with around 700,000 points in the point cloud.

2.2 Rockbolt information extraction

To perform condition monitoring of the rockbolts, information regarding their position on the tunnel surface, and their protruding length is required. By performing a comparison of this information extracted from multiple point cloud scans, the condition of individual rockbolts can be evaluated. Extraction of information of individual rockbolts from the point cloud is performed in a series of steps and these are described briefly as follows:

- Point cloud data quality evaluation: The point cloud data within the same organisation can be acquired through different LiDAR devices and this impacts the quality of the data. Also, since the LiDAR acquires the surface data through reflected beams, the density of the points depends on the distance of the surface from the device. Finally, the density of the point cloud also depends on the reflectivity of the surface. Various algorithms used for processing the point cloud data are dependent on the neighbourhood distance values of the point cloud data, hence an initial evaluation of the nearest neighbour distance is performed and is used as a parameter for algorithms in the data processing pipeline.
- Point cloud voxelisation: Voxelisation segments the point cloud data based on virtual cuboids in 3D space. This is required since storage of individual points in point cloud data does not correspond to the relative positioning of the points in the real world. Voxelisation is used to extract a neighbourhood of points for analysis. In this paper, a voxel of side length 40 cm is created using the library function available in Open3D, since protruding rockbolt size had been observed to be less than this value.
- Voxel surface extraction: The set of points extracted within the voxel represent a small region of the tunnel surface. A plane is fitted to the extracted set of points. This results into two sets of points inliers and outliers. Inliers are the set of points lying within a threshold of the plane and outliers are the set of points lying beyond the threshold. The threshold is based on the standard deviation of the surface of the point cloud and computed during the point cloud quality evaluation phase. Also, the fitted plane is used to generate a surface normal and inlier points are used to generate a surface centroid.
- Outlier clustering: The outlier is a set of points representing the objects on the tunnel surface beyond the inlier threshold value where the inlier represents the tunnel wall. This includes rockbolts, steel mesh, steel ribs, power cables and ventilation pipes. After removing the inliers, the outlier points are clustered using density-based spatial clustering of applications with noise (DBSCAN) clustering (Ester et al. 1996). DBSCAN requires nearest neighbour distance as a parameter and depends on the point cloud data quality. This value is computed during the initial data quality evaluation stage. This creates disjointed clusters representing the objects near the tunnel surface.
- Cluster evaluation: Some of the formed clusters may represent rockbolts, hence the clusters are evaluated individually. A set of criteria that describes a rockbolt's representation in point cloud data

was developed. The criteria evaluate the number of points, length of the cluster along its principal axis, angle between the principal axis of the cluster and the inliers plane surface normal, and finally the minimum distance between the cluster and the surface plane. Each cluster is evaluated based on each of the previously mentioned criteria. The clusters that satisfy all the criteria have the set of points representing the rockbolts.

- Rockbolt surface position extraction: At this stage, the remaining clusters are the rockbolts. The position of the rockbolt on the surface is extracted by computing the point of intersection between the principal axis of the cluster and the plane surface.
- Rockbolt tip position extraction: The farthest point in the cluster from the plane surface is saved as the rockbolt tip position. A combination of the rockbolt surface position and tip position provides the protruding length and the orientation of the rockbolt.
- Rockbolt data export: The data extracted from the previous computation is saved for future computations. The following information for each rockbolt is exported: surface normal, surface centroid, surface point, and tip point.

2.3 Rockbolt condition monitoring

After the LiDAR scan is performed, the point cloud data is processed and rockbolt data is extracted as described in the previous section. The time and region of interest are selected based on the logged microseismic events. Condition monitoring of rockbolt data is performed by processing the point cloud data and extracted rockbolt information from two consecutive scans surrounding a microseismic event. In this paper the two scans will be called the previous scan and the latest scan for clarity. The condition monitoring of the rockbolt is performed based on rockbolt protruding length and change in orientation with respect to the tunnel surface. The data processing steps required to perform rockbolt condition monitoring are described in this section.

Data import: At this stage, point cloud data and the rockbolt information associated to the point cloud data as exported from the previous stage are available. Based on the logged microseismic events time and location, two scans and rockbolt information are loaded as the previous and the latest data sets.

Registration error quantification: Underground tunnels are a GPS denied environment, i.e. absolute localisation is not possible due to lack of GPS signals. Relative localisation is performed as per the mine coordinate system. Surveyors perform the LiDAR scanning and localise the point cloud to the mine coordinate system with the help of markers located on the tunnel surface. This process is called the registration of the point cloud. Registration may result in a small error in the positioning of the point cloud. This error has six degrees of freedom, i.e. translation and rotational errors along the three axes. Also, this error is spatially variable along the tunnel surface. Since the rockbolts will be compared to their counterparts in other scans, quantification of registration error is required for the entire tunnel surface.

Local registration error between two point cloud surfaces can be measured by using the M3C2 algorithm (Lague et al. 2013). M3C2 algorithm is applied as follows:

1. A key point representing the location is selected in first point cloud.
2. A set of points within a given radius R, forming a neighbourhood are selected (R depends on the surface variability).
3. A surface normal for this set of points is computed, i.e. perpendicular to the surface created by the set of point.
4. A second set of points within a radius r and centre at the key point are selected such that $r < R$.
5. The second set of points are projected on to the surface normal and mean and standard deviation of the projected points are computed.

6. For the second point cloud, the points within the radius r around the surface normal are selected and the mean and standard deviation of the projected points is computed.

Figure a shows the two point clouds, the key point and r being the radius of the cylinder. Figure b shows the surface normal (as described in M3C2 algorithm) as the axis of the cylinder and the distribution of the projected points from the two points clouds.

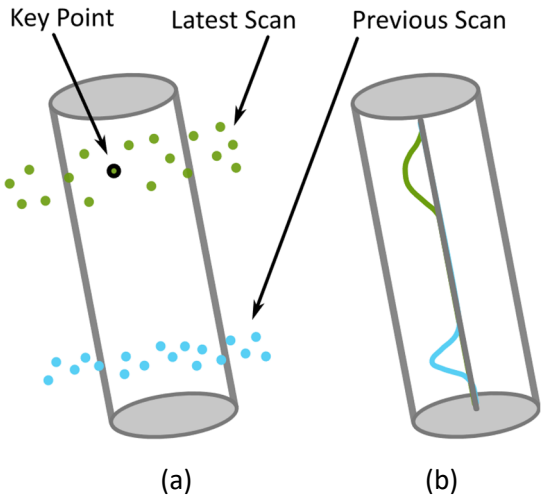

Figure 1 Comparison of two point cloud surfaces. (a) Two point clouds, the key point and r (radius of cylinder); (b) Surface normal as the axis of the cylinder and the distribution of the projected points

To apply the above algorithm to a tunnel, some modifications are required. The voxels as a region within R, their surface normal, and surface centroids as key points have been used to apply the M3C2 algorithm. The key points and surface normal computed for the latest scan are used for the computation. Figure shows a part of the point cloud. The cuboids represent the direction of the surface normal and the points within the cuboid are used to compute the distribution of the points.

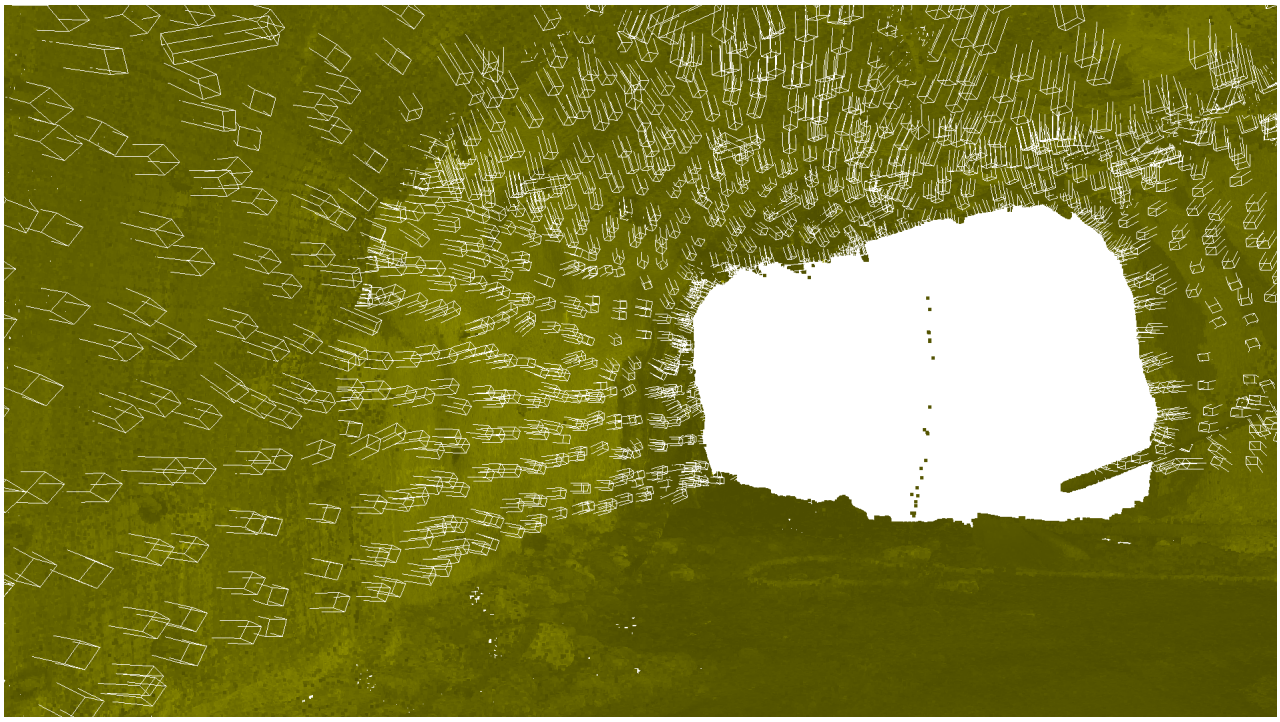

Figure 2 Locations used for computation of local registration error

Figure 3a shows the distribution of points for the latest and the previous scans at a single location. Figure 3b shows the histogram of differences between the mean values for all the locations. It can be observed from Figure 3b that the distribution is confined between ±0.025 m and this represents the local registration error between the surfaces of the two point clouds.

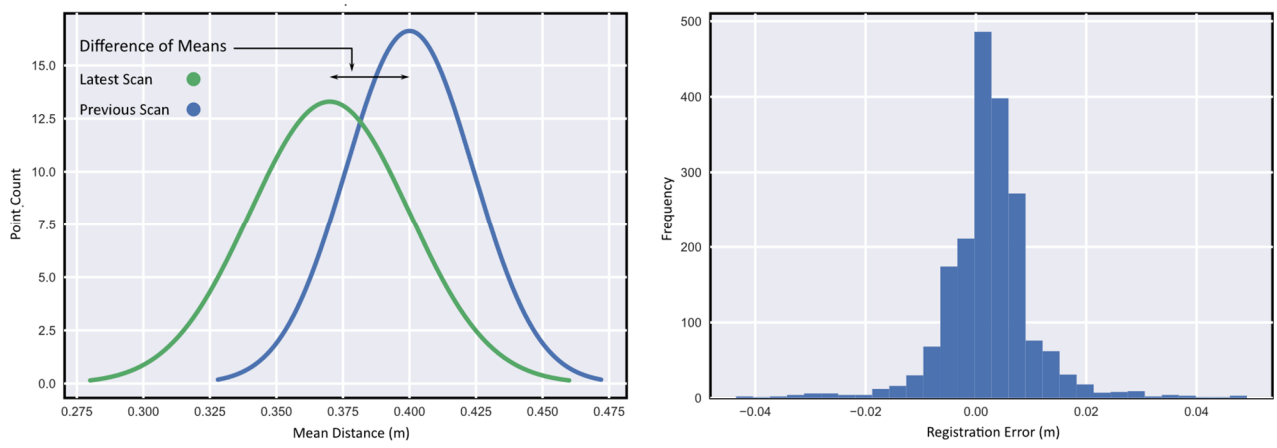

(a) (b)

Figure 3 Measurement of surface distance. (a) Latest and previous surface point distribution at a single point; (b) Histogram of difference of mean computed at all the locations

Rockbolt pairing: To extract the condition of a rockbolt over time, individual rockbolt information from two point cloud scans has to be extracted. To establish one on one correspondence between the rockbolts from two scans, the Euclidian distance between all the rockbolt surface points obtained from the latest and previous scan are computed. In the previous step, it was observed that the spread of registration error was ±0.025 m, as seen in Figure 3b. Hence, to compensate for the registration error, rockbolts with their surface point pairs with the distance less than 0.05 m are retained. It should be observed that the Euclidian distance between the rockbolts should be within ±0.025 m. The value was doubled to compensate for errors along six degrees of freedom. Also, since the rockbolts are not installed within 0.05 m of each other, this will not lead to any errors in identifying the corresponding rockbolts.

It was observed that one-on-one correspondence for all the rockbolts was not generated in the previous step and this can be due to the fact that rehabilitation is performed on a regular basis due to the instability of the region.

Rockbolt length comparison: For all the corresponding rockbolts detected from the two scans, a protruding length comparison is performed. Since, for each rockbolt, the surface point and the tip point had been exported, the difference of these two values is the length of each rockbolt. It should be noted that since the rockbolt length is computed between the surface and tip point of the rockbolt, it is not affected by the registration error.

Rockbolt orientation comparison: Similar to the previous step, the orientation of each rockbolt is computed as a vector between the surface and tip point. The angle between the corresponding rockbolts is computed using the dot product between the orientation vectors.

Deformation in area between the bolts: Presence of rockbolts in the form of ground support should reduce the deformation. However, the regions farthest from the rockbolts can be of interest to determine the need for rehabilitation based on cumulative deformation. Extraction of deformation information for the farthest regions is carried out as follows:

1. For the detected rockbolts in the latest scan, a mesh is generated such that the rockbolt surface positions are the vertices of the triangles formed in the mesh, as seen in Figure 4.

2. Rockbolt neighbourhood area and centroid computation are computed for each triangle that is formed in the mesh with the vertices as the rockbolt surface points.

The area is used to filter large triangles which may be formed in open spaces (based on outliers from standard deviation). The centroid location is used to compute the surface-to-surface distance between the two point clouds and a correction is applied based on the average registration error from the three vertices of the triangle (rockbolt surface positions).

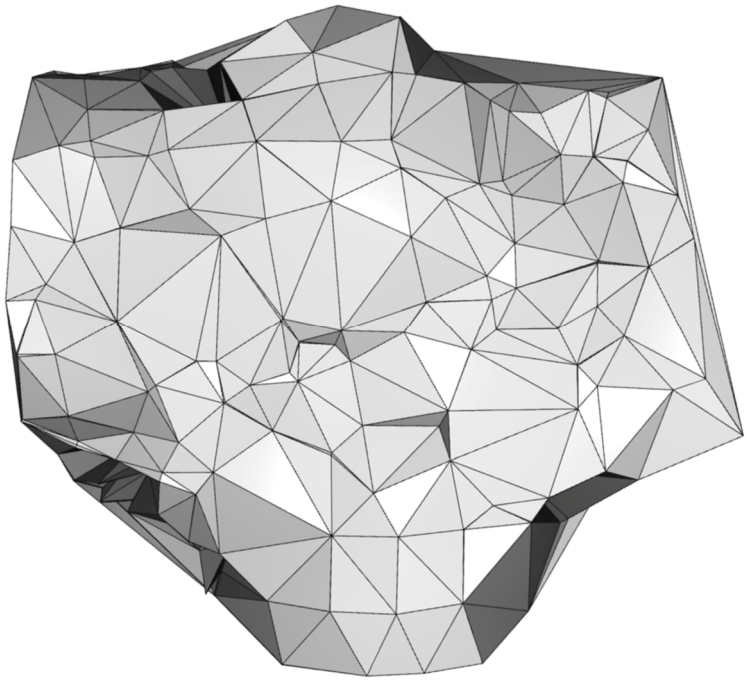

Figure 4 Mesh of tunnel surface with rockbolts as vertices

2.4 Visualisation

Underground tunnels, and hence the collected data such as the blasting, microseismic events and the point cloud data, correspond to the events in 3D space. To provide the best possible representation of the extracted information and support the decision-making process, suitable visualisations should be created. In this paper, visualisations have been tested in three mediums: on computer screens for quick result evaluation, in virtual reality (VR) environment for offsite immersive visualisation, and in augmented reality environment (AR) for onsite comparative visualisation. All the figures discussed in this section are captured from 3D interactive visualisations. This allows the user to change the orientation and scale of the visual output to aid in the interpretation of the results.

2.4.1 Point cloud visualisation for rockbolt comparison

Figure 5 represents the change in rockbolt length. The cones in red represent convergence while the cones in blue represent divergence. The direction of the cone is aligned with the direction of the rockbolt in the latest scan. It should be noted that the orientation of the blue cone is opposite to that of the red cones indicating opposite direction (2D projection loses the pose/transformation information). The cones have been scaled 300% since the small difference in rockbolt length is very small as compared to tunnel scale. Further, to improve the visibility, the set of cones have been scaled 105%, and this positions the cones outside the point cloud data.

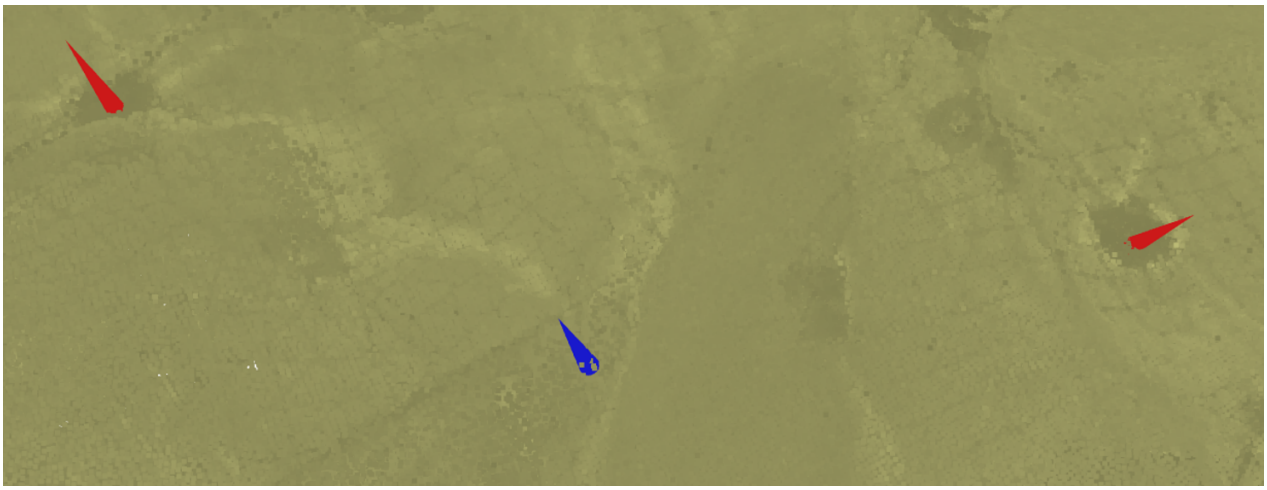

Figure 5 Rockbolt length difference markers on tunnel surface

2.4.2 Point cloud visualisation for spatial error

Figure shows the computed mean surface error between the two scans. The computation of difference of mean of surface distribution is discussed in the previous section. The computed value is represented as spheres positioned at the location of computation, and the radius of the sphere is the difference of means. The red spheres represent convergence while the blue spheres represent divergence. The sphere radii have been scaled 300% for visualisation.

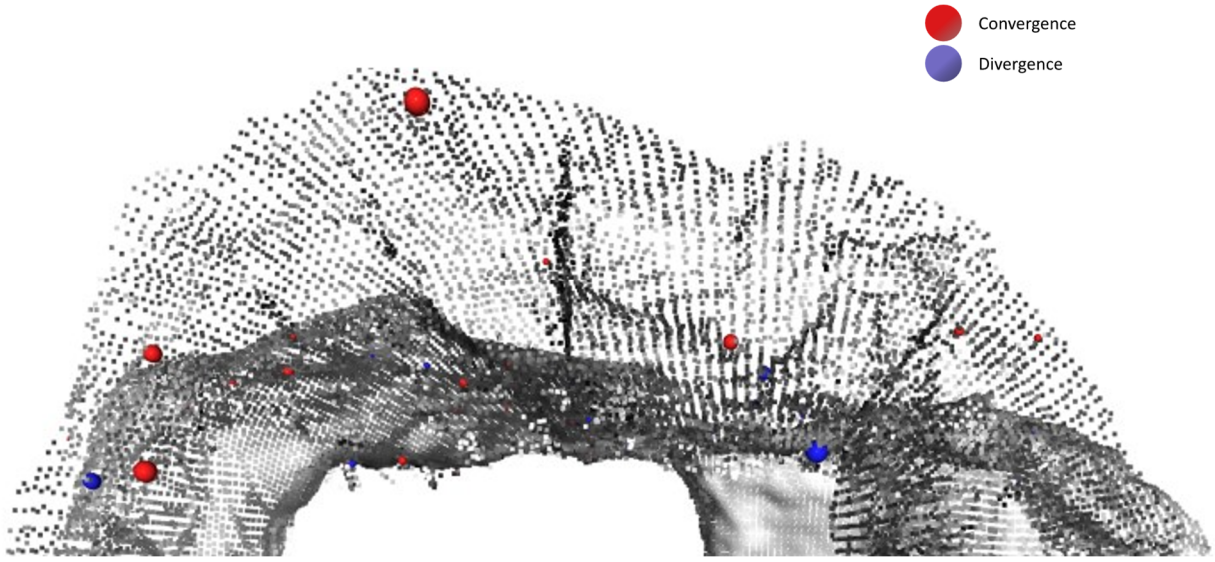

Figure 6 Computed registration error over the surface of the tunnel shown as low density point cloud

2.4.3 Neighbourhood visualisation with mesh model

In addition to visualisation of rockbolt length difference within the point cloud, the length difference is also visualised on the surface mesh model, as seen in Figure 4 for the mesh based tunnel representation and Figure 7 which shows a close-up with tunnel mesh and rockbolt length difference represented as a cone. The structure of the mesh is generated using the position of the rockbolts on the tunnel surface. Higher density mesh representation is possible by using more tunnel surface points. The advantage of this method is that the mesh model requires small storage space. The point cloud based model requires about 500 MB of storage space, whereas the mesh-based model requires about 100 KB. Additionally, the mesh-based model can be visualised with many 3D visualisation software systems as well as in web browsers. Mesh-based visualisations are suitable for long-term storage, requiring less storage while containing most of the required information.

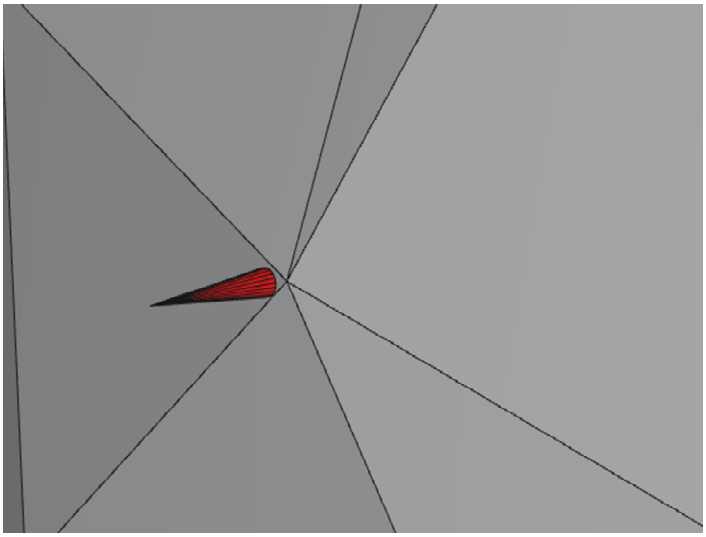

Figure 7 Rockbolt difference on surface mesh model

2.4.4 Point cloud visualisation with virtual and augmented reality

A VR-based environment allows the user to load the point cloud data where the detected rockbolts are highlighted in red. This interface allows the user to visualise the condition with high resolution with scaling and orientation is under the user's control, as seen in Figure 8. This kind of visualisation can be useful for offsite inspection with overlays showing the results of computation.

An AR environment can load the same marked point cloud and will allow it to overlap with a digital image of the real-world location to allow comparison. This is suitable for on-site inspection when the results of computation can be overlayed on to the physical structures.

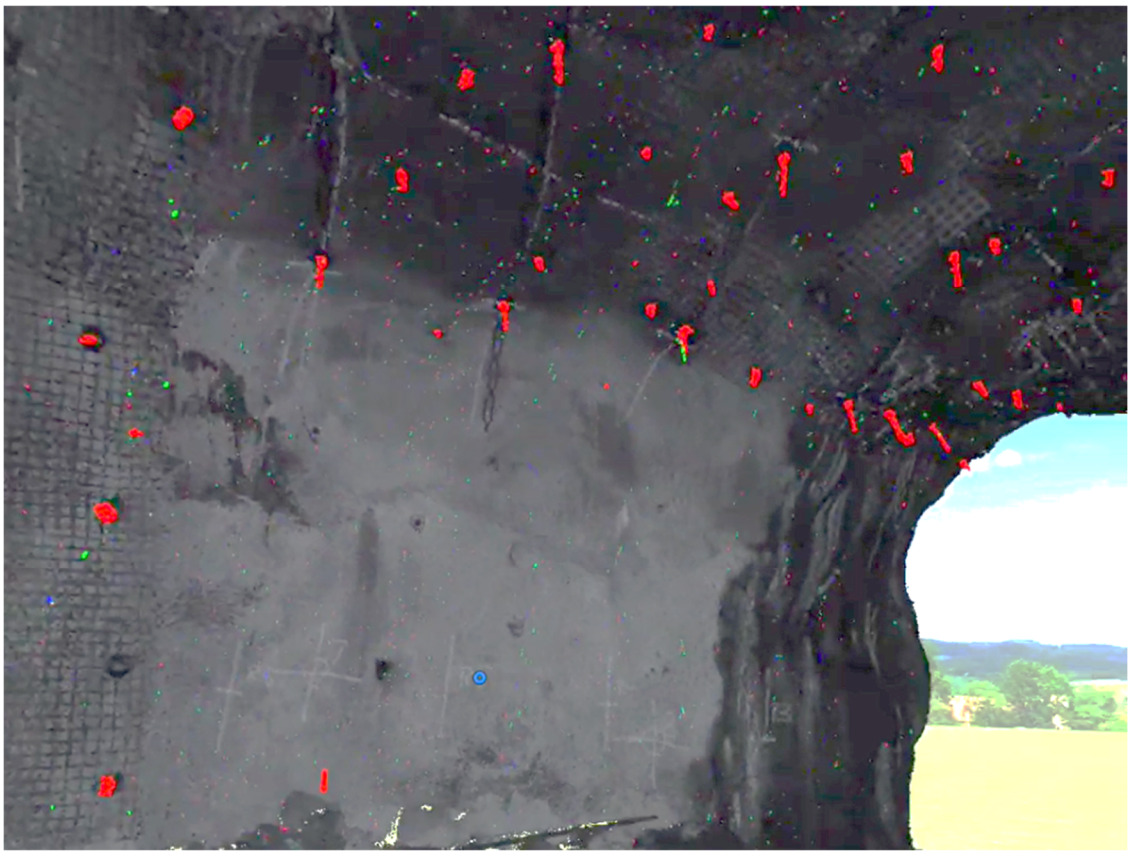

Figure 8 Tunnel point cloud data with highlighted rockbolts in virtual reality environment

3 Conclusion

This paper presents a methodology for extraction of rockbolt information from point cloud data representing underground drifts. Rockbolt information such as rockbolt protruding length, the position on the surface, angle to the surface, etc. are extracted. The extracted information is used to compare the rockbolt condition over time. Also, a method for quantification of registration error between point clouds is presented and this information is used to evaluate the deformation in unsupported areas between the rockbolts. Finally, 3D interactive visualisations are created to be used by the mining engineers as a decision support tool.

The discussed workflow utilises available data sets such as the point cloud data, surveying information, blasting, microseismic event time, and locations, and applies point cloud processing techniques to add value to already available methods. The data processing workflow is developed in Python programming language with open-source libraries. The data processing workflow has been developed as an end-to-end automated process and does not require any user intervention. The end-to-end processing of a point cloud (~ 13 million points) to extract rockbolt information requires less than 20 minutes of computation time on a normal laptop. Subsequent processing and visualisations require less than 1 minute each. The developed algorithms can scale very efficiently to use parallel computation.

The following conclusions were drawn from this work:

1. Point cloud data may have variability in term of density and quality. Hence, evaluation of point cloud data and its quantification is required to perform comparison between point cloud data sets.
2. Rockbolt representation with two points, i.e. the surface and tip point, are an efficient and effective representation. This representation has been used to extract a wealth of information like (but not limited to) the protruding length of the rockbolt, angle between the rockbolt and tunnel surface, and the changes to the inter-rockbolt neighbourhood. While performing comparison of point clouds, the two-point rockbolt representation helps in determining the rockbolt counterparts, computing of protruding length difference, and change in orientation by comparison of angle.
3. Point cloud data based monitoring provides information for all the surfaces and assets in the tunnel including the tunnel surface, ground support, pipes, cables, and equipment. Automation of monitoring based on point cloud data allows the engineers to focus on the regions of interest based on experience or based on automated monitoring.
4. Visualisation of comparison of registration error over the tunnel surface and difference in rockbolt lengths can be seen as a band spread over the tunnel surface. This provides a visual guide for condition monitoring of ground support and in turn guides the need for rehabilitation in the marked areas. However, 2D projection of 3D structures can result in a loss of information and can be partially compensated for by using interactive visualisation. VR-based and AR-based visualisation supports depth perception in addition to control over orientation and scale. Use of VR and AR for offsite or on-site inspection and monitoring can improve the monitoring process in terms of time, accuracy, and overall safety.
5. Since post-processing exports the rockbolt information, an incremental database of rockbolts (date of scan and rockbolt information) can be created through successive scans. This will incorporate the rehabilitation information into rockbolt condition monitoring and streamline integration with other data sources.
6. Rockbolt movement along its length is one indicator of loss of function, which can be determined from the discussed point cloud processing workflow. However, inclusion of other features is required to develop trigger action response plans. These include, but not limited to, rockbolt type yielding/non-yielding, structural model, and numerical model.

3.1 Limitations

Limitations within this work are in the form of failure in detection of rockbolts that have a short length on the surface. This occurs since one of the rockbolt evaluation factors discards any cluster having height less than a set threshold (< 0.03 m). This is a recurring issue reported by other researchers, hence a methodology for detection of short rockbolts on tunnel surface can be explored.

Detection of rockbolts depends on its surface properties. When the rockbolts are rusted, the number of points detected on their surface is reduced. Reduced number of points on the rockbolt decreases the accuracy during protruding length detection. As can be seen in Figure 8, the surface markings are clearly visible. Painting the rockbolts with similar paint (visible region, painted off-white) before or during the installation can increase their visibility in point cloud. Use of different means of colouring the points can also be helpful, such as using the reflectance to improve point cloud data quality.

Registration of point cloud data sets using the extracted rockbolt positions can reduce registration error. Standard registration methods relying on large number of points and features are not able to reduce registration error. Registration methods capable of performing registration with small number of points and able to utilise orientation information can be explored to reduce this error.

3.2 Future work

Each process of extraction of rockbolts information, comparison of rockbolts, computation of protruding length difference and deformation, and finally, the registration error, have been developed as individual modules. The processing can be scaled horizontally through use of cloud computing to reduce the required computation time and to deal with larger amounts of data.

The discussed methodology provides a data-driven technique to perform condition monitoring of the ground support while utilising information from other data sources. Extensive knowledge is available based on material, structural properties and physics-based modelling such as finite element methods. However, this information is mostly available within the software used within the organisations. Additionally, knowledge of mining engineers and surveyors about the site is a valuable source for assessing the site. One of the approaches towards integration of multi-domain, multi-source data, and information is through creations of digital twins. A hybrid digital twin supports integration of data sources and physics-based models. This can lead to improved results as compared to when any of the methods is used alone.

Acknowledgement

This project was carried out under the funding received from Mining Innovation for Ground Support (MIGS). The authors would like extend their deepest appreciation to the domain experts from various organisations associated with the MIGS consortium for sharing their knowledge and experience. The authors would also like to acknowledge Ms. Linnea Nordin for her support in development of VR and AR environments for improving usability of the results. Finally, the authors are thankful to the reviewers for through and insightful comments.

References

Ester, M, Kriegel, H, Xu, X & Miinchen, D 1996, 'A density-based algorithm for discovering clusters in large spatial databases with noise', *KDD-96: Proceedings of the Second International Conference on Knowledge Discovery and Data Mining*, AAAI Press, Portland.

Fernandes, D, Silva, A, Névoa, R, Simões, C, Gonzalez, D, Guevara, M … & Melo-Pinto, P 2021, 'Point-cloud based 3D object detection and classification methods for self-driving applications: a survey and taxonomy', *Information Fusion*, vol. 68, pp. 161–191, https://doi.org/10.1016/j.inffus.2020.11.002

Gallwey, J, Eyre, M & Coggan, J 2020, 'A machine learning approach for the detection of supporting rock bolts from laser scan data in an underground mine', *Tunnelling and Underground Space Technology*, vol. 107, https://doi.org/10.1016/j.tust.2020.103656

Gigli, G & Casagli, N 2011, 'Semi-automatic extraction of rock mass structural data from high resolution LIDAR point clouds', *International Journal of Rock Mechanics and Mining Sciences*, vol. 48, pp. 187–198, https://doi.org/10.1016/j.ijrmms.2010.11.009

Harris, CR, Millman, KJ, van der Walt, SJ, Gommers, R, Virtanen, P, Cournapeau, D … Oliphant, TE 2020, 'Array programming with {NumPy}', *Nature*, vol. 585, pp. 357–362, https://doi.org/10.1038/s41586-020-2649-2

Jones, EW 2020, 'Mobile LiDAR for underground geomechanics: learnings from the teens and directions for the twenties', in J Wesseloo (ed.), *UMT 2020: Proceedings of the Second International Conference on Underground Mining Technology*, Australian Centre for Geomechanics, Perth, pp. 3-26, https://doi.org/10.36487/ACG_repo/2035_0.01

Jones, E & Beck, D 2018, 'The use of three-dimensional laser scanning for deformation monitoring in underground mines', *Proceedings of the 13th Underground Operators' Conference*, Australasian Institute of Mining and Metallurgy, Melbourne.

Lague, D, Brodu, N & Leroux, J 2013, 'Accurate 3D comparison of complex topography with terrestrial laser scanner: application to the Rangitikei canyon (N-Z)', *ISPRS Journal of Photogrammetry and Remote Sensing*, vol. 82, pp. 10–26, https://doi.org/10.1016/j.isprsjprs.2013.04.009

Leottau, DL, Vallejos, P & Ruiz, J 2020, LIDAR-based displacement estimation in mining applications, *Automining 2018: 6th International Congress on Automation in Mining*, Gecamin, Santiago.

Li, CC 2017, 'Principles of rockbolting design', *Journal of Rock Mechanics and Geotechnical Engineering*, vol. 9, pp. 396–414, https://doi.org/10.1016/j.jrmge.2017.04.002

Li, S, Yue, D, Zheng, D, Cai, D & Hu, C 2022, 'A geometric-feature-based method for automatic extraction of anchor rod points from dense point cloud', *Sensors*, vol. 22, no. 23, https://doi.org/10.3390/s22239289

Martínez-Sánchez, J, Puente, I, González-Jorge, H, Riveiro, B & Arias, P 2016, 'Automatic thickness and volume estimation of sprayed concrete on anchored retaining walls from terrestrial LIDAR data', *ISPRS Journal of Photogrammetry and Remote Sensing*, vol. 41, pp. 521–526, https://doi.org/10.5194/isprsarchives-XLI-B5-521-2016

Poux, F, Neuville, R, Van Wersch, L, Nys, GA & Billen, R 2017, '3D point clouds in archaeology: Advances in acquisition, processing and knowledge integration applied to quasi-planar objects', *Geosciences*, vol. 7, no. 4, https://doi.org/10.3390/geosciences7040096

Romero-Jarén, R & Arranz, JJ 2021, 'Automatic segmentation and classification of BIM elements from point clouds', *Automation in Construction*, vol. 124, https://doi.org/10.1016/j.autcon.2021.103576

Rusu, RB, Blodow, N & Beetz, M 2009, 'Fast Point Feature Histograms (FPFH) for 3D Registration', *Proceedings of the 2009 IEEE International Conference on Robotics and Automation*, IEEE, Kobe, pp. 3212–3217. https://doi.org/10.1109/ROBOT.2009.5152473

Sakurai, S 1984, 'Displacement measurements associated with the design of underground openings', Proceedings of the International Symposium on Field Measurements in Geomechanics, A.A. Balkema, Rotterdam, pp. 1163–1178.

Saydam, S, Liu, B, Li, B, Zhang, W, Singh, SK & Raval, S 2021, 'A coarse-to-fine approach for rock bolt detection from 3D point clouds', *IEEE Access,* vol. 9, pp. 148873–148883, https://doi.org/10.1109/ACCESS.2021.3120207

Simser, BP 2007, 'The weakest link - ground support observations at some Canadian shield hard rock mines', in Y Potvin (ed.), *Deep Mining 2007: Proceedings of the Fourth International Seminar on Deep and High Stress Mining*, Australian Centre for Geomechanics, Perth, pp. 335–348, https://doi.org/10.36487/ACG_repo/711_25

Singh, SK, Raval, S & Banerjee, B 2021a, 'A robust approach to identify roof bolts in 3D point cloud data captured from a mobile laser scanner', *International Journal of Mining Science and Technology*, vol. 31, no. 2, pp. 303–312, https://doi.org/10.1016/j.ijmst.2021.01.001

Singh, SK, Raval, S & Banerjee, B 2021b. 'Roof bolt identification in underground coal mines from 3D point cloud data using local point descriptors and artificial neural network', *Remote Sensing*, vol. 42, pp. 367–377, https://doi.org/10.1080/2150704X.2020.1809734

Van Rossum, G 1995, *Python Tutorial*, Centrum voor Wiskunde en Informatica, Amsterdam.

Walton, G, Diederichs, MS, Weinhardt, K, Delaloye, D, Lato, MJ & Punkkinen, A 2018, 'Change detection in drill and blast tunnels from point cloud data', *International Journal of Rock Mechanics and Mining Sciences*, vol. 105, pp. 172–181, https://doi.org/10.1016/j.ijrmms.2018.03.004

Weinmann, M, Weinmann, M, Mallet, C & Brédif, M 2017, 'A classification-segmentation framework for the detection of individual trees in dense MMS point cloud data acquired in urban areas', *Remote Sensing*, vol. 9, pp. 0–28, https://doi.org/10.3390/rs9030277

Xue, F, Lu, W, Chen, Z & Webster, CJ 2020, 'From LiDAR point cloud towards digital twin city: Clustering city objects based on Gestalt principles', *Journal of Photogrammetry and Remote Sensing*, vol. 167, pp. 418–431. https://doi.org/10.1016/j.isprsjprs.2020.07.020

Yu, H, Lu, X, Cheng, G & Ge, X 2011, 'Detection and volume estimation of mining subsidence based on multi-temporal LiDAR data', *Proceedings of the 19th International Conference of Geoinformatics*, IEEE, Shanghai, https://doi.org/10.1109/GeoInformatics.2011.5980892

Yu, H, Lu, X, Ge, X & Cheng, G 2010, 'Digital terrain model extraction from airborne LiDAR data in complex mining area', *Proceedings of the 18th International Conference of Geoinformatics*, IEEE, Beijing, https://doi.org/10.1109/GEOINFORMATICS.2010.5567781

Zhou, Q-Y, Park, J & Koltun, V 2018, *Open3D: A Modern Library for 3D Data Processing*, Cornell University, Ithaca, arXiv.org/abs/1801.09847